



Anatomical description of the skulls of peccaries (*Tayassu tajacu*, Linnaeus 1758) by computed tomography

[Descrição anatômica de crânio de catetos (*Tayassu tajacu*, Linnaeus, 1758) por tomografia computadorizada]

J.R. Araújo¹, R.P.S. Rodrigues¹, F.C.A. Sousa², L.S. Moura¹, A.B.S. Silva¹,
G.T. Pessoa¹, K.V. Macedo¹, F.S. Costa³, K.R.S. Leitão¹,
P.V.S. Carvalho¹, F.R. Alves^{2*}

¹Aluno de pós-graduação - Universidade Federal do Piauí - Teresina, PI

²Universidade Federal do Piauí - Teresina, PI

³Universidade Federal Rural de Pernambuco - Recife, PE

ABSTRACT

The aim of this study was to evaluate the anatomical structures of the skulls of peccaries to establish the basis for their clinical study and future preclinical research. Ten skulls of adult peccaries were subjected to tomographic examination. The data obtained were processed via three-dimensional image reconstruction software (3D images). The reconstructions obtained from the neurocranium of the studied specimens allowed the identification and description of the following structures: nasal bone, frontal bone, parietal bones, incisor bone, maxillary bone, zygomatic bone, temporal bone, palatal bone, occipital bone, vomer bone, pterygoid bone, sphenoid bone, paranasal sinuses and orbit. Computed tomography proved to be an important diagnostic tool in the investigation of the skull of this species, allowing the acquisition of anatomical values not yet documented for the species in the literature.

Keywords: imaging diagnosis, neurocranium, *Tayassuidae*, wild animals

RESUMO

O objetivo deste estudo foi avaliar as estruturas anatômicas dos crânios de catetos, a fim de se estabelecerem as bases para seu estudo clínico e futuras pesquisas pré-clínicas. Dez crânios de catetos adultos foram submetidos a exame tomográfico. Os dados obtidos foram introduzidos em um software de reconstrução de imagens tridimensionais (imagens em 3D). As reconstruções obtidas do neurocrânio dos espécimes estudados permitiram a identificação e a descrição das seguintes estruturas: osso nasal, osso frontal, ossos parietais, osso incisivo, osso maxilar, osso zigomático, osso temporal, osso palatino, osso occipital, osso vômer, osso pterigoide, osso esfenóide, seios paranasais e órbita. A tomografia computadorizada mostrou-se como uma ferramenta diagnóstica importante na investigação do crânio dessa espécie, permitindo a aquisição de valores anatômicos ainda não documentados para a espécie na literatura.

Palavras-chave: diagnóstico por imagem, neurocrânio, *Tayassuidae*, animais silvestres

INTRODUCTION

Peccaries (*Tayassu tajacu*) are wild suiformes that belong to the order Artiodactyla, family Tayassuidae and genus *Tayassu* (Orr, 1986). These animals live in diverse habitats from the southwestern United States to Argentina. With

an excellent sense of smell, the peccary can locate, by scent, plant bulbs to a substantial depth and then use their snout to dig and retrieve them (Bodmer and Sowls, 1993; Miller and Fowler, 2012). Computed tomography is used in many animals for the study of the head and, especially, evaluation of the paranasal sinuses (Alsafy *et al.*, 2013). In humans, it is a well-established and

Received on August 10, 2020

Accepted on December 1, 2020

*Author for correspondence (*corresponding author*)

E-mail: flavioribeiro@ufpi.edu.br

well-recognized diagnostic imaging tool; in companion animals and wild species, it has been more widely used in recent years, contributing to improved prognoses and more effective treatment plans (Capello and Cauduro, 2008).

Accurate knowledge of the craniofacial anatomy of swine together with an understanding of the different imaging modalities help to improve radiologists' ability to distinguish normal and abnormal anatomic characteristics (Kyllar *et al.*, 2014). The diversity of cranial bones reflects biomechanical adaptations related to feeding and morphological, biomechanical, ecological and phylogenetic aspects (Kamminga *et al.*, 2017). The objective of this study was to evaluate the anatomical structures of the skulls of peccaries to establish the bases for their practical clinical study and future preclinical research. The results of this study will contribute singularly to the understanding of the cranial morphology of this wild species. In addition, these findings will serve as a basis for improved diagnostic approaches and will favor the development of more effective clinical surgical approaches that will aid in the ecological preservation of these suiformes.

MATERIAL AND METHODS

Ten uniformly sized skulls of adult peccaries (*Tayassu tajacu*, Linnaeus, 1758) were used. The anatomical pieces comprise the bone collection of the Animal Anatomy Laboratory of the Veterinary Morphology Department of the Agricultural Sciences Center of the Federal University of Piauí, Teresina, Piauí, Brazil. The protocols used in this study were approved by the Committee on Ethics in Animal Experimentation - EAA/UFPI (No. 415/17) and authorized by the Ministry of the Environment, through the System of Authorization and Information of Biodiversity - SISBIO of the Brazilian Institute of the

Environment and Renewable Natural Resources - IBAMA (N^o 60348).

Computed tomography was performed at a Veterinary Imaging Diagnostic Center located in Recife, Pernambuco, Brazil. Helical tomography equipment (Hi-Speed FXI, General Electric (GE), Japan) was used with a radiation emitting channel of 120 kVp and auto-mA at a speed of one s-1 rotation. To obtain the tomographic images, the skulls were placed on an examination table that moves into the interior of the porch, at which point the scout is performed (rostral portion of the incisive bone to the caudal portion of the occipital bone), and an image similar to conventional radiography is captured. The data obtained (raw data) were processed with an image reconstruction program to format the various reformatting plans. Computed tomography images in the axial, sagittal and coronal planes were stored as digital imaging and communications in medicine (DICOM) images for posterior analysis and bone description.

RESULTS

The bones of the skull of the peccaries form a sheath of rigid tissue that surrounds soft tissues such as the brain and the organs of smell, sight and hearing and serve to support the external organs that make up the respiratory and digestive systems. The neurocranium of these animals belonging to the order Artiodactyla was evaluated by computed tomography, and the following bones were described: nasal, frontal, parietal, incisive, maxillary, zygomatic, temporal, palatine, occipital, vommer, pterygoid, sphenoid, paranasal sinus and orbital. The skulls of the peccaries as a whole presented uniformity among the evaluated specimens, being long and with an almost rectilinear frontal profile (Figures 1, 2 and 3).

Anatomical description...

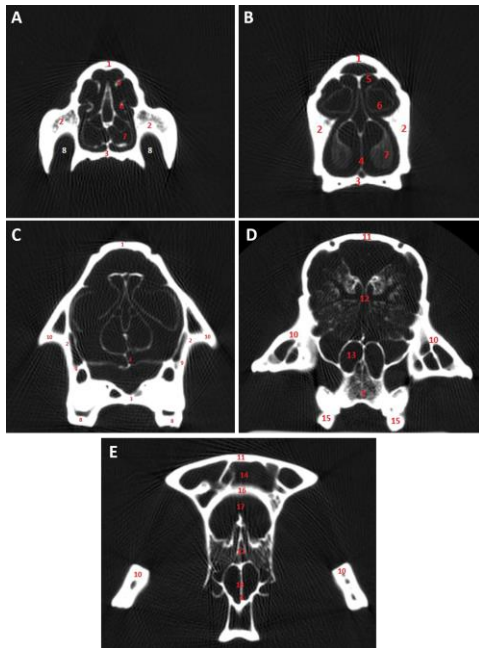


Figure 1. Axial computed tomography (CT) images of the peccary (*Tayassu tajacu*, Linnaeus 1758) skull. [A-F] 1 - Nasal bone; 2 - Maxillary bone; 3 - Palatal bone; 4 - Vomer bone; 5 - Dorsal nasal concha; 6 - Medial nasal concha; 7 - Ventral nasal concha; 8 - First molar tooth; 9 - Maxillary sinuses; 10 - Zygomatic bone; 11 - Frontal bone; 12 - Ethmoidal labyrinth; 13 - Choanal region; 14 - Frontal sinuses; 15 - Third molar tooth; 16 - Calvaria; 17 - Cerebral cavity; 18 - Nasopharyngeal meatus; 19 - Temporal bone; 20 - Tympanic bulla.

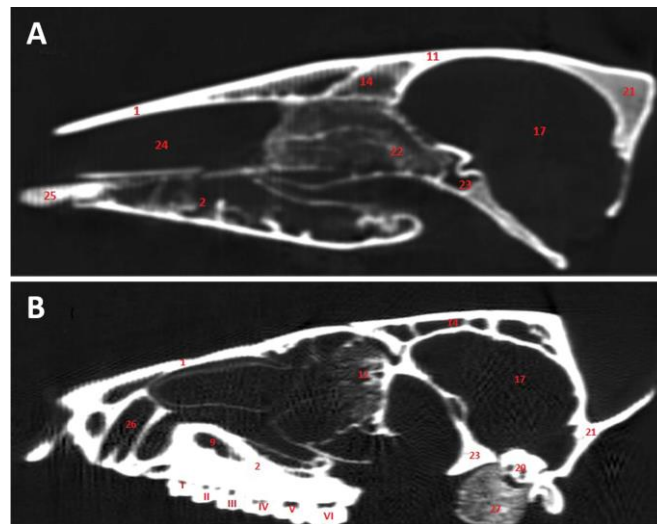


Figure 2. Sagittal computed tomography images of the peccary (*Tayassu tajacu*, Linnaeus 1758) skull. [A - medial sagittal image; B - lateral sagittal image] 1 - Nasal bone; 2 - Maxillary bone; 3 - Palatal bone; 4 - Vomer bone; 5 - Dorsal nasal concha; 6 - Medial nasal concha; 7 - Ventral nasal concha; 8 - First molar tooth; 9 - Maxillary sinuses; 10 - Zygomatic bone; 11 - Frontal bone; 12 - Ethmoidal labyrinth; 13 - Choanal region; 14 - Frontal sinuses; 15 - Third molar tooth; 16 - Calvaria; 17 - Cerebral cavity; 18 - nasopharyngeal meatus; 19 - Temporal bone; 20 - Tympanic bulla; 21 Occipital bone; 22 - Ethmoid bone (turbinate); 23 - Sphenoid; 24 - Nasal cavity; 25 - Incisive bone; 26 - Canine tooth alveolus; 27- Temporal bone; 28 - Supraorbital foramen; I - First molar tooth; II - Second molar tooth; III - Third molar tooth; IV - Fourth molar tooth; V - Fifth molar tooth; VI - Sixth molar tooth.

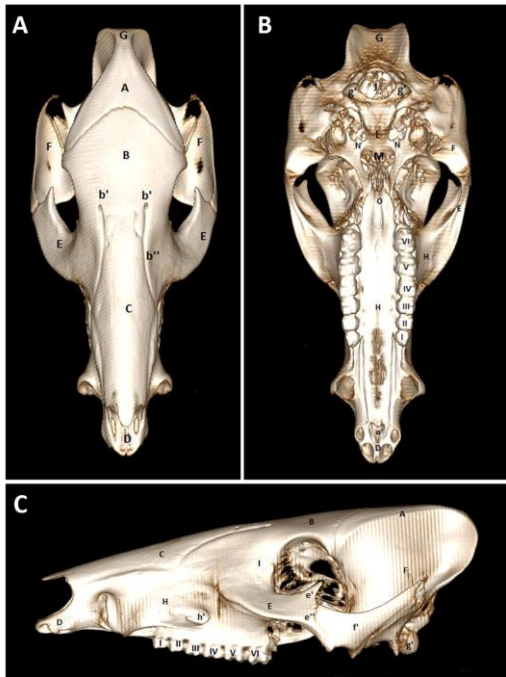


Figure 3. Computed tomography images of the peccary (*Tayassu tajacu*, Linnaeus 1758) skull. Images of three-dimensional reconstruction in the dorsal (A), ventral (B) and lateral (C) directions. A - Parietal bone; B - Frontal bone; C - Nasal bone; D - Incisive bone; E - Zygomatic bone; F - Temporal bone; G - Occipital bone; H - Maxillary bone; I - Lacrimal bone; J - Foramen magnum; L - Basisphenoid bone; M - Vomer; N - Pterygoid bone; O - Palatal bone; b' - Supraorbital foramen; b'' - Supraorbital groove; e' - Frontal process of the zygomatic bone; e'' - Temporal process of the zygomatic bone; f' - Zygomatic process of the temporal bone; g' - Occipital condyle; h' - Infraorbital foramen; o'' - Cleft palate; I - First molar tooth; II - Second molar tooth; III - Third molar tooth; IV - Fourth molar tooth; V - Fifth molar tooth; VI - Sixth molar tooth.

In multiplanar images, the tomographic study showed superior quality in soft tissue window delimiting with better clarity regarding the architecture of fine bones. Sagittal sections showed the insertion point of the nostrils by the meatus and nasal conchae, the site of nasal canal debouchment in the frontal and maxillary sinuses, and the differentiation of ethmoid and ethmoturbinate bones. The nasal cavity extends into the extension of the frontal sinus and nasomaxillary opening, which expands laterally to the maxillary sinus. Nasal bones (Figure 1) have a longiline anatomical shape and internally form a considerable part of the nasal cavity roof. Its syntopy is related rostrally with articulation of the incisive bones, laterally with the maxillary bones and caudally with the frontal bone. Nasal conchae are thin walled and have a low-density spiral shape. The nasal septum reaches the floor of the nasal cavity delimiting the sinus and dorsal nasal concha, the middle nasal concha and the ventral nasal concha.

The incisive bone (Figure 2) is even and forms the most rostral extension (except rostral bone) of the bony skull. This bone has one body and three processes (alveolar, nasal and palatal) that articulate with the nasal bone and maxillary and indirectly with the rostral bone. The fusion of the paired bones is incomplete along the midline, resulting in a narrow fissure called the interincisive that is amenable to evaluation in multiplanar coronal images. The maxillae are the main bones of the upper jaw; they support the upper molar teeth and are located on the lateral surface of the face and articulate with the incisive bone (rostrally), nasal bone (dorsomedially), frontal bone (caudodorsomedially), lacrimal bone (caudally), zygomatic bone (caudolaterally), palatine bone (caudoventromedially), ethmoid bone (medially) and ventral nasal concha (internally). They are extensive and form a considerable part of the lateral wall of the nasal cavity. It is possible to visualize the dental alveolus and teeth (one

Anatomical description...

canine tooth, three premolar teeth and three molar teeth in each antimer) in sagittal, axial and coronal tomographic images as well as reconstructions of the three-dimensional images.

The temporal bones form a significant part of the lateral wall of the caudal cranial fossa. Each bone is located between the occipital bone (caudally), the parietal bone (dorsally), the frontal bone (rostrodorsally), and the basisphenoid bone (rostroventrally). In peccaries, it consists of three distinct parts: scaly, tympanic and petrous. The pair of frontal bones is interposed between the parietal bones (caudally, parietal margin) and nasal bones (rostrally, nasal margin). They articulate with the ethmoid bone, lacrimal bone, wings of the presphenoid and basisphenoid, jawbone and squamous part of the temporal bone. They are irregular and consist of squamous, nasal and orbital parts.

The vomer is a medium and long bone that assists in the formation of the ventral part of the nasal septum. Its rostral end approaches the incisor bone body and is pointed out. Caudally, it extends to the level of the presphenoid. It is distinctly grooved (septal groove) on its dorsal surface to receive cartilage from the nasal septum and caudally receives the bone perpendicular blade of the ethmoid bone. The ethmoid bone is located deep inside the skull between the cranial and facial parts. It is situated between the right and left orbital fossae and partially surrounded by excavations of the nasal cavity. It consists of paired labyrinths (lateral masses), orbital and ridding blades, pairs, and a perpendicular blade. The pterygoid bones are paired and articulate with the palatal bone, with the pterygoid process of the basisphenoid bone and with the vomer. The lateral surface is free ventrally and forms the medial wall of the pterygopalatine fossa. Its medial face is smooth and forms the caudal limit of the nasopharyngeal meatus, osseous.

The palatine bones are located on both sides of the choanal region (caudal nostrils) and form the caudal part of the hard palate. Each one articulates with the bone on the opposite side, with the maxilla, and with the pterygoid, basisphenoid, vomer, presphenoid and ethmoid bones. Each is folded to form a horizontal, perpendicular blade. The lacrimal bones are located on the rostral margin of the osseous orbit,

have irregular shapes and articulate with the maxilla, zygomatic, ethmoid, frontal, and, to a limited extent, the nasal bones and ventral concha. The zygomatic bone is dorsoventrally wide and compressed mediolaterally; it has a broad and slightly convex lateral surface, competing rostrally with the maxilla and lacrimal bones in the formation of the muscular fossa, which is limited by the facial ridge.

The parietal bones are even. The parietal plane is medially limited where it joins the bone on the opposite side; the sagittal margin is short and straight. Rostrally, the parietal bones attach to the frontal bone in the long and curved frontal margin; caudally, they attach extensively to the occipital bone at the occipital margin. The temporal plane forms a large part of the temporal fossa; caudally, it joins the occipital bone in the formation of the distinct nuchal ridge and is ventrally covered by the squamous part of the temporal bone on the extensive scaly margin. The orbit of peccaries is formed by the frontal and sphenoid bones in its dorsal portion; ethmoid, sphenoid and lacrimal bones in its medial wall; maxillary, zygomatic and palatine bones in its ventral portion; and zygomatic and sphenoid bones in its lateral portion (presenting incomplete). Three-dimensional reconstruction of tomographic images helps in the detailed identification of cranial bones of peccaries (Figure 3), allowing greater clarity and acuity in the identification of bone surfaces and accidents.

DISCUSSION

In the present study, computed tomography provided excellent spatial resolution of the bone tissue of the skulls of peccaries. This advanced imaging diagnostic technique has been used to evaluate the heads of humans (Capello and Cauduro, 2008), horses (D'Août *et al.*, 2015; Gonçalves *et al.*, 2015; Liuti *et al.*, 2017), buffaloes (Alsafy *et al.*, 2013), canines (Rycke *et al.*, 2003), pigs (Kyllar *et al.*, 2014), felines (Losonsky *et al.*, 1997), and goats (Moawad *et al.*, 2017), among others. Our observations coincide with the descriptions made by Kyllar *et al.* (2014) in pigs but differ from those of other domestic species due to phylogenetic, taxonomic, food and ecological distance. Analysis of the results of this study indicates that all bone structures of the peccary skull can be evaluated by computed tomography.

Household swine are widely used in preclinical medical research as an animal model because of their anatomical and physiological characteristics that can be extrapolated to other species, including humans (Pemberton *et al.*, 2005). Currently, there is a study by Kyllar *et al.* (2014) describing the diagnostic imaging anatomy of the craniofacial region of the domestic pig. Thus, we focus our attention on cranial tomographic studies of peccaries to provide a description of the normal anatomy, which can be applied in experimental studies of structures such as the nasal cavity, paranasal sinuses, cranial nerves, eyes, teeth, and other facial structures.

Computed tomography is used less frequently in veterinary medicine than radiography; however, its widespread use is becoming more common, especially in small animals (Losonsky *et al.*, 1997). The cost of CT scans hinders their routine use in clinical or experimental settings. On the other hand, it is possible to generate diagnostic images by computed tomography in different planes, providing radiologists with detailed anatomical information, spatial orientation, visualization of structures in the neurocranium that are obscured in radiographs, and excellent visualization of the temporomandibular joint, orbit and middle ear (Rycke *et al.*, 2003).

The use of a three-dimensional reconstruction program is another advantage of computed tomography that allows the evaluation of the spatial orientation of the head; on the other hand, it is limited only to the bony parts of the skull (Kammaing *et al.*, 2017). In our study, the skulls were positioned symmetrically, resulting in the acquisition of symmetrical transverse (axial) tomographic images that were 1.5 mm thick. The tomographic images showed the bone structures numerically identified in axial, sagittal and three-dimensional reconstructions. The peccary skulls evaluated in this study were similar in size, shape, opacity and relation of anatomical structures to each other. Dogs (Rycke *et al.*, 2003, Lorigados and Pinto, 2013) and cats tend to have different anatomical relationships of structures due to the great variation in the shape of the skulls. Thus, it can be assumed that brachycephalic dogs and cats, for example, would present differences in the anatomical relationships of the nasal cavity and paranasal sinuses in comparison to dolichocephalic and tablexphalic races. Such cranial variation was

not observed in the skulls studied since wild species have uniform body regions when compared to each other.

The conformation of the canine head reflects the appearance of specific changes in each format. Chronic nasal disease has been reported more frequently in dolichocephalic dogs. CT scans greatly enhance the ability to diagnose chronic nasal disease in dogs, providing detailed information on the extent of disease and accurate discrimination of neoplastic and nonneoplastic diseases (Lefebvre *et al.*, 2005). In peccaries, it is not currently possible to associate the shape of the skull with a specific disease since these wild specimens do not have the cranial variation observed in the different breeds of dogs and cats.

One of the major difficulties of experimental studies is the transposition of their results for application in humans. This should be done cautiously, without precipitous conclusions since any results obtained are absolute truths only for the animal species studied (Venter *et al.*, 2005). In peccaries, future research is necessary, preferably carried out on live animals under sedation, to eliminate possible errors of interpretation. In addition, taking into account the nonexistence of clinical studies that compare different diagnostic imaging methods in the diagnostic evaluation of the head of these wild animals, subsequent studies are essential for clinical practice in this species, without any risk to patients.

CONCLUSION

Computed tomography proved to be a viable technique in the anatomical study of the skull in peccaries. Swine is an animal routinely used as preclinical models, due to its physiological similarities to humans. In this context, peccaries are presented for the first time in an advanced study of tomographic image of the skull. The results found for the anatomy of the skull of this animal generated information applicable to Veterinary Medicine of wild animals, as well as an option of animal model for studies that can be extrapolated to humans.

ACKNOWLEDGMENTS

The Coordination for the Improvement of Higher Education Personnel (CAPES), for the award of the Doctorate Scholarship.

REFERENCES

- ALSAFY, M.A.M.; EL-GENDY, S.A.A.; SHARABY, A.A.E. Anatomic reference for computed tomography of paranasal sinuses and their communication in the Egyptian buffalo (*Bubalus bubalis*). *Anat. Histol. Embryol.*, v.42, p.220-231, 2013.
- BODMER, R.E.; SOWLS, L.K. In status survey and conservation action plan: pigs peccaries and hippos. Gland, Switzerland: IUCN, 1993. 202p.
- CAPELLO, V.; CAUDURO, A. Clinical technique: application of computed tomography for diagnosis of dental disease in the rabbit, guinea pig, and chinchilla. *J. Exotic Pet. Med.*, v.17, p.93-101, 2008.
- D'AOÛT, C.; NISOLLE, J.F.; NAVEZ M. *et al.* Computed tomography and magnetic resonance anatomy of the normal orbit and eye of the horse. *Anat. Histol. Embryol.*, v.44, p.370-377, 2015.
- GONÇALVES, R.; MALALANA, F.; MCCONNELL, J.F. *et al.* Anatomical study of cranial nerve emergence and skull foramina in the horse using magnetic resonance imaging and computed tomography. *Vet. Radiol. Ultrasound*, v.56, p.391-397, 2015.
- KAMMINGA, P.; BRUIN, P.W.; GELEIJNS, J. *et al.* X-ray computed tomography library of shark anatomy and lower jaw surface models. *Sci. Data*, v.4, p.1-6, 2017.
- KYLLAR, M.; STEMBÍREK, J.; PUTNOVÁ, I.; M. Radiography, computed tomography and magnetic resonance imaging of craniofacial structures in pig. *Anat. Histol. Embryol.*, v.43, p.435-452, 2014.
- LEFEBVRE, J.; KUEHN, N.F.; WORTINGER A. *et al.* Computed tomography as an aid in the diagnosis of chronic nasal disease in dogs. *J. Small. Anim. Pract.*, v.46, p.280-285, 2005.
- LIUTI, T.; REARDON, R.; DIXON, P.M. Computed tomographic assessment of equine maxillary cheek teeth anatomical relationships, and paranasal sinus volume. *Vet. Rec.*, v.181, p.452-458, 2017.
- LORIGADOS, C.A.B.; PINTO, A.C.B.F. Tomografia computadorizada do encéfalo do cão: aspectos da normalidade e correlação anatômica. *Arq. Bras. Med. Vet. Zootec.*, v.65, p.729-734, 2013.
- LOSONSKY, J.M.; ABBOTT, L.C.; KURIASHKIIN, I.V. Computed tomography of the normal feline nasal cavity and paranasal sinuses. *Vet. Radiol. Ultrasound*, v.38, p.251-258, 1997.
- MILLER, R.E.; FOWLER, M.E. *Zoo & wild animal medicine*. 2.ed., Philadelphia: W. B. Saunders, 2012. 970p.
- MOAWAD, U.K.; AWAAD, A.S.; ABEDELLAAH, B.A. Morphological, histochemical and computed tomography on the vomeronasal organ (Jacobson's organ) of Egyptian native breeds of goats (*Capra hircus*). *J. Basic Appl. Sci.*, v.6, p.174-183, 2017.
- ORR, R.T. *Biologia dos vertebrados*. 5.ed. San Francisco-California: Academy of Sciences, 1986. 242p.
- PEMBERTON J.; LI X.; KARAMLOU C.A.; SANDQUIST K. *et al.* The use of live three-dimensional Doppler echocardiography in the measurement of cardiac output: na in vivo animal study. *J. Am. Coll. Cardiol.*, v.45, p.433-438, 2005.
- RYCKE, L.M.; SAUNDERS, J.H.; GIELEN, I.M. *et al.* Magnetic resonance imaging, computed tomography, and cross-sectional views of the anatomy of normal nasal cavities and paranasal sinuses in mesaticephalic dogs. *Am. J. Vet. Res.*, v.64, p.1093-1098, 2003.
- VENTER, N.G.; JAMEL, N.; MARQUES, R.G. *et al.* Avaliação de métodos radiológicos na detecção de corpo estranho de madeira em modelo animal. *Acta. Cir. Bras*, v.20, p.19-26, 2005